ILL-POSEDNESS OF ABSORBING BOUNDARY CONDITIONS APPLIED ON CONVEX SURFACES.

DANIEL NORELAND

Abstract. Absorbing boundary conditions are important in many applications where partial differential equations defined on infinite domains are solved numerically. A problem that has attracted interest recently is that perfectly matched layers layers (PML) for electro-magnetic FDTD simulations applied on convex surfaces may lead to instabilities. This paper shows that these problems are not restricted to electro-magnetic calculations, but common for problems described by the classical wave equation with absorbing boundary conditions on convex surfaces. It is shown that the instabilities are independent of the numerical implementation of the absorbing boundary condition, and instead a result of unphysical assumption in the formulation of the boundary condition.

1. Introduction. Absorbing boundary conditions (ABC:s) are used in computational applications in order to simulate domains of infinite extension. Computational acoustics and computational electro-magnetics are examples of broad areas where absorbing boundary conditions are widely used. For wave phenomena, four classes of boundary conditions are most common; sponge layers, Sommerfeld radiation equations, Engquist-Majda conditions and perfectly matched layers layers (PML). For an overview of the vast topic of ABC:s, the reader is referred to a review article by Tsynkov [8].

Apart from questions regarding implementation and computational complexity, the property of absorbing boundary conditions that has attracted the most interest is their reflection coefficients. A much less regarded factor is the influence of the shape of the boundary conditions on the stability properties of the mathematical and numerical models. A fact that deserves attention is the observation that an ABC cannot be applied on a boundary of arbitrary shape, and give physically acceptable solutions.

The fact that converging spherical waves inside cones may give rise to unstable time-domain simulations has previously been observed for so-called *digital-waveguide* models of wind instruments[1]. A digital waveguide is a one-dimensional bidirectional delay-line, used for sound synthesis. It is not until recently that this problem of spherical waves has been associated to the field of numerical boundary conditions, however. In a number of studies by Teixeira ([5], [6] and [7]) of non-Cartesian PML:s for electro-magnetic computations, it is shown that the proposed implementations of PML:s lead to instability when applied on convex boundaries. In this paper, it is shown that this property of ABC:s is fundamental for waves governed by the linear wave equation, and not in any respect associated to the specific implementation of the ABC. The experiments accounted for in this paper refer to a particular implementation of an ABC, but the results are relevant for other implementations.

The phenomena of interest in this paper are governed by the scalar, linear wave equation in a homogeneous medium,

$$\frac{\partial^2 p(\mathbf{x},t)}{\partial t^2} = c^2 \Delta p(\mathbf{x},t)\,, \tag{1}$$

where $p(\mathbf{x},t)$ is the acoustic pressure at position $\mathbf{x}$ at time t, c is the velocity of sound and Δ denotes the Laplacian operator. Electro-magnetic waves are generally more complicated, but can in many cases be described by an equation like Eqn. (1). The results of this paper should therefore be relevant also for such simulations.

The wave equation turns into the Helmholtz equation when expressed in the frequency domain. The usual way to do this is to assume a time dependence of the form $\exp(i\omega t)$, which leads to the equation[1]

$$(c^2\Delta + \omega^2)p = 0, \quad \omega \in \mathbb{R}.$$

The time dependence $\exp(i\omega t)$ is usually associated with the Fourier transform, which is defined for $\omega \in \mathbb{R}$. Although it is possible to extend the definition to also include complex values of ω, it is customary to instead write the time dependence as $\exp(st)$, $s \in \mathbb{C}$, in which case the transition from time-domain to frequency domain is obtained using the Laplace transform. The Helmholtz equation therefore has the form

$$(c^2\Delta - s^2)p = 0, \quad s \in \mathbb{C}$$

in most part of this paper.

The concept of well posedness for partial differential equations has been quite extensively studied. Although the special problem presented in this paper may be investigated using the methods in e.g [3], a slightly different stance is taken here, using some concepts from linear control theory. Also, the definition of well posedness used in [3] is somewhat sharpened in order to better suite physical properties of the problems at hand. The definition of well-posedness in [3] allows solution with a growth of the type $\exp(\alpha t)$, $\alpha > 0$. However, for a physical system described by the homogeneous wave equation with homogeneous boundary conditions, the acoustic energy is not allowed to grow in time. For this reason, the term *unstable* refers, in this paper, to continuous problem formulations with the property that acoustic energy grows in time in an unphysical way.

2. Converging spherical waves. This section presents the behaviour of a convex, absorbing boundary from a control theory aspect. Part of the argument in this section involves the acoustic *input impedance*. This entity is usually defined in the ω-domain, and in order to comply with the established notation in acoustics, a time dependence $\exp(i\omega t)$ is initially assumed, with the addition that also complex ω are allowed. The transition to the s-domain is straightforward. Consider the waveguide of Fig. 1. It is a cone truncated by spherical end caps at $r = R_1$ and $r = R_2$, where r is the distance from the apex of the cone. Assuming a time dependence $\exp(i\omega t)$, the scalar, linear wave equation gives rise to a Helmholtz equation, which in spherically polar coordinates has the form

$$\frac{1}{r^2}\frac{\partial}{\partial r}\left(r^2\frac{\partial p}{\partial r}\right) + \frac{1}{r^2 \sin\theta}\frac{\partial}{\partial \theta}\left(\sin\theta\frac{\partial p}{\partial \theta}\right) + \frac{1}{r^2\sin^2\theta}\frac{\partial p}{\partial \phi^2} + k^2 p = 0, \tag{2}$$

where $k = \omega/c$. At the lateral surface of the cone, the sound-hard boundary condition $\partial p/\partial\theta = 0$ is imposed. At the boundary $r = R_1$ an ABC is imposed. For the moment, let the exact form of this boundary condition be unspecified. The requirement from it is that it has the property of being perfectly absorbing, or *anechoic*, in the sense that any wave front impinging on it from the interior of Ω, leaves the domain without reflection. Considering only waves of the type $p = p(r)$, that is spherically symmetric

[1] Since the distinction is clear from the context, variables in the frequency domain are, in this paper, denoted by the same symbol as in the time domain.

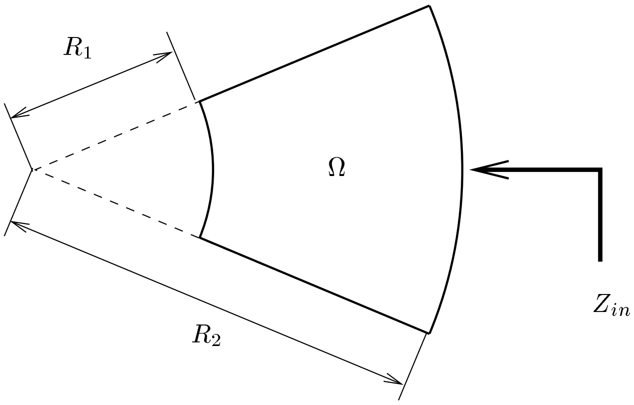

FIG. 1. *A converging waveguide.*

waves, Eqn. (2) reduces to

$$\frac{\partial^2 p}{\partial r^2} + \frac{2}{r}\frac{\partial p}{\partial r} + k^2 p = 0. \tag{3}$$

As a consequence of the linearity of the governing differential equation, the reduction to one dimension makes it possible to write $p(\omega)$ at $r = R_2$ as a constant times the particle velocity $v(\omega)$ at the same position. Therfore no specific boundary condition is prescribed at the right boundary. Instead, we study the input impedance $Z_{in}(\omega) = p(\omega)/U_{in}(\omega)|_{R_2}$ seen from $r = R_2$, looking to the left. Here, U_{in} is the acoustic volume inflow given by $U_{in} = Sv_{in}$, where S is the wave front area, and v_{in} is the particle velocity with respect to an inward pointing normal. Borrowing the terminology from control theory, the input impedance is the transfer function from U_{in} to p_{in}, or equivalently, the Fourier transform of the impulse response in p. In the absence of a boundary condition at $r = R_2$, the solution to (3) should not be regarded as the solution of a specific problem. Instead, Z_{in} is itself a boundary condition that represents the domain Ω and could be used for the solution of the Helmholtz equation *to the right* of R_2.

The solutions to (3) are of the form

$$p(r) = A\frac{e^{-ikr}}{r} + B\frac{e^{ikr}}{r}.$$

With a perfectly absorbing boundary condition at $r = R_1$, all right travelling waves are cancelled, implying that $A = 0$. The relation between the acoustic pressure and the particle velocity $\mathbf{v}$ is given by the linearised momentum balance equation

$$\varrho\frac{\partial \mathbf{v}(\mathbf{x},t)}{\partial t} = -\nabla p(\mathbf{x},t).$$

In the frequency domain, we have for $\mathbf{v}(\mathbf{x},\omega)$ that

$$\mathbf{v}(\mathbf{x},\omega) = \frac{i}{\omega\varrho}\nabla p(\mathbf{x},\omega),$$

or, for the radial component v in the spherically symmetric case,

$$v(r,\omega) = \frac{i}{\omega\varrho}\frac{\partial p(r,\omega)}{\partial r}.$$

In the example above we thus have, with $A = 0$ and $B = 1$,

$$v(r, \omega) = -\frac{1}{\varrho c}\frac{e^{ikr}}{r} - \frac{i}{\varrho\omega}\frac{e^{ikr}}{r^2}.$$

According to the established definition of Z_{in}, the acoustic volume flow U_{in} should be calculated with respect to an *inward* pointing normal. Thus,

$$Z_{in} = \left.\frac{p}{Sv_{in}}\right|_{R_2} = \left.\frac{p}{-Sv}\right|_{R_2} = \frac{1}{S}\frac{\frac{e^{ikR_2}}{R_2}}{\frac{1}{\varrho c}\frac{e^{ikR_2}}{R_2} + \frac{i}{\varrho\omega}\frac{e^{ikR_2}}{R_2^2}} = \frac{1}{S}\frac{\varrho c}{1 + \frac{i}{kR_2}}.$$

Whence,

$$Z_{in}(\omega) = \frac{\varrho c}{S}\frac{i\omega}{i\omega - \frac{c}{R_2}}. \tag{4}$$

In the s-domain, we have

$$\tilde{Z}_{in}(s) = \frac{\varrho c}{S}\frac{s}{s - \frac{c}{R_2}}, \tag{5}$$

where the tilde denotes the change of argument. Once a transfer function of a system has been established, the corresponding impulse response $h(t)$ can be computed by forming the inverse Fourier transform of the transfer function. For the system at hand we have

$$h(t) = \mathcal{F}^{-1}Z_{in}(\omega) = \frac{\varrho c}{S}[\delta(t) - \frac{c}{R_2}e^{ct/R_2}\Theta(-t)],$$

where $\Theta(t)$ denotes the Heaviside step function;

$$\Theta(t) = \begin{cases} 0, & t < 0 \\ 1, & t \geq 0. \end{cases}$$

Now, the appearance of the term $\Theta(-t)$ suggests that the impulse response of the system would be a signal that starts *before* the input signal is fed into the system. Such a system is termed *anti causal*, and is obviously not a feasible model of a physical system. The core of the problem is the pole of Z_{in} that appears at $i\omega = c/R_2$. Although the wave equation itself is inherently causal in the sense that the signal speed is finite, this is not a property that carries over automatically to any problem formulated in the frequency domain when boundary conditions are prescribed. However, we know *a priori* that any valid model should represent a causal system. Furthermore, a numerical time domain simulation of an equation originally stated in the frequency domain will necessarily constitute a causal system – whether the original frequency domain model is causal or anti causal. In reality, the causality of a system is determined by the integration contour along which the inverse transform of the transfer function is computed.

In control theory, it is often more convenient to work with the Laplace transform instead of the Fourier transform, since the former is defined for a larger class of functions, including also signals with an exponential growth. The calculation of the inverse Laplace transform requires knowledge of the region of convergence (ROC) of the transform. The ROC determines on which side of the poles of $Z_{in}(s)\,, s = i\omega$ the integration path will pass. For a signal with support on $t \geq 0$, which is the result of a causal system, the ROC is the half plane to the right of the rightmost pole. For such signals, the transform of choice is the *unilateral* Laplace transform, as opposed to the *bilateral* Laplace transform, which is the closest relative to the Fourier transform. With this choice of the ROC the inverse Laplace transorm of Eqn. (5) yields the impulse response

$$h(t) = \mathcal{L}^{-1}\tilde{Z}_{in}(s) = \frac{\varrho c}{S}\left(\delta(t) + \frac{c}{R_2}e^{ct/R_2}\Theta(t)\right),$$

which is causal, but exponentially growing.

The pole located at c/R_2 approaches origo of the s-plane as R_2 increases. For a domain Ω truncated far from the apex of the cone, the possible instability is thus a low frequency phenomenon. In the limit $R_2 \to \infty$, the pole $s \to 0$, and the input impedance attains the constant value $\varrho c/S$, which is the impedance of a duct of constant cross-sectional area.

In light of the foregoing discussion, the following can be stated; *If a physically feasible boundary condition can be described by a rational transfer function, it must have neither poles nor zeros with a positive real part.* Remark: Such a system is commonly denoted *minimum phase.* This is a most natural condition, since both Z_{in} and Z_{in}^{-1} must be stable transfer functions, or simply put, a passive acoustic component cannot generate energy whether a pressure or a volume flow velocity is fed into it.

The appearance of a pole in the right half plane indicates that a boundary condition of the discussed type is potentially dangerous. A growth of the type $\exp(\alpha t)$ will occur if the instability is triggered. Whether this is the case or not is, as the next section will show, depending on the other boundary conditions of the problem.

3. One-dimensional model examples. In this section, three simple one-dimensional model examples are investigated. The examples are seemingly very similar, but the small differences are of crucial importance to the stability of the problems. The geometry of interest is again a truncated cone as in Fig. 1, or a sphere, in which axially symmetric waves are considered. Due to the symmetry, wave propagation in the waveguide is governed by the equation

$$\frac{1}{c^2}\frac{\partial^2 p}{\partial t^2} = \frac{\partial^2 p}{\partial r^2} + \frac{2}{r}\frac{\partial p}{\partial r}. \tag{6}$$

The constant $c = 1$ was chosen for notational convenience only. Common to the three problems is that on the boundary $r = R_1$, a version of the first order spherical outflow condition introduced eg. by Engquist and Majda[2] is imposed. The condition is modified to be applied on a convex surface instead of a concave surface, as in the original paper. The boundary condition, that takes the form

$$\frac{\partial p}{\partial t} = \frac{\partial p}{\partial r} + \frac{p}{R_1}, \quad r = R_1,$$

allows for converging spherical wave fronts to leave Ω without reflection. This is simply seen by inserting an inward travelling spherical wave of the form $p(r,t) = f(r+ct)/r$ into the boundary condition. On the boundary $r = R_2$, three different boundary conditions are investigated. They are, in turn, sound-hard, absorbing and open.

3.1. Sound-hard right boundary. Consider the problem

$$\frac{\partial^2 p}{\partial t^2} = \frac{\partial^2 p}{\partial r^2} + \frac{2}{r}\frac{\partial p}{\partial r}, \quad R_1 < r < R_2 \tag{7a}$$

$$\frac{\partial p}{\partial t} = \frac{\partial p}{\partial r} + \frac{p}{R_1}, \quad r = R_1 \tag{7b}$$

$$\frac{\partial p}{\partial r} = 0, \quad r = R_2\,. \tag{7c}$$

The Neumann condition at $r = R_2$ models a sound-hard boundary.

Applying the method of separation of variables, the solutions to Eqn. (7) are written on the form $p(r,t) = R(r)T(t)$. Assuming a time dependence

$$T(t) = e^{st},$$

it is seen that the radial part $R(r)$ of the solution to Eqn. (7a) satisfies the equation

$$R'' + \frac{2}{r}R' - s^2 R = 0. \tag{8}$$

Together with the boundary conditions (7b) and (7c), Eqn. (8) defines an eigenvalue problem, whose eigenvalues and eigensolutions determine the stability of the problem. The solutions of Eqn. (8) are spherical Bessel function of the 0:th order, or put in the often more convenient exponential notation,

$$R(r) = A\frac{e^{-sr}}{r} + B\frac{e^{sr}}{r}. \tag{9}$$

The question is now if there are any non-trivial solutions to Eqn. (7) with $\mathrm{Re}(s) \geq 0$. Such solutions indicate non-vanishing or growing components of the solution. Inserting (9) into the left boundary condition yields

$$s\left(A\frac{e^{-sR_1}}{R_1} + B\frac{e^{sR_1}}{R_1}\right) =$$
$$-A\frac{se^{-sR_1}}{R_1} - A\frac{e^{-sR_1}}{R_1^2} + B\frac{se^{sR_1}}{R_1} - B\frac{e^{sR_1}}{R_1^2} + A\frac{e^{-sR_1}}{R_1^2} + B\frac{e^{sR_1}}{R_1^2}\,,$$

or

$$s\left(A\frac{e^{-sR_1}}{R_1} + B\frac{e^{sR_1}}{R_1}\right) = -A\frac{se^{-sR_1}}{R_1} + B\frac{se^{sR_1}}{R_1}. \tag{10}$$

The right boundary condition, in turn, yields

$$-A\frac{se^{-sR_2}}{R_2} - A\frac{e^{-sR_2}}{R_2^2} + B\frac{se^{sR_2}}{R_2} - B\frac{e^{sR_2}}{R_2^2} = 0. \tag{11}$$

Equation (10) requires that $s = 0$ or $A = 0$, but leaves B arbitrary. The case $s = 0$ has to be treated separately, since then the two components of Eqn. (9) collapse to the same solution. Equation (11) together with $A = 0$ gives

$$B\frac{se^{sR_2}}{R_2} - B\frac{e^{sR_2}}{R_2^2} = 0.$$

The non-trivial solutions non-trivial solutions require that

$$\frac{se^{sR_2}}{R_2} = \frac{e^{sR_2}}{R_2^2}$$

or

$$s = \frac{1}{R_2}.$$

For $s = 0$, it is readily seen that the general solution to Eqn. (8) is given by

$$R(r) = C + \frac{D}{r}, \tag{12}$$

but only the trivial solution $C = 0$, $D = 0$ satisfies Eqn. (7b) and (7c). With

$$R(r) = B\frac{e^{\frac{r}{R_2}}}{r},$$

we finally have

$$p(r,t) = B\frac{e^{\frac{r+t}{R_2}}}{r},$$

which shows that Eqn. (7) has an exponentially growing solution. The fact that the growth speed is independent of R_1 is a result of the ABC imposed here.

In Fig. 9, the time evolution of a spherical pulse travelling to the left can be seen. The simulation was computed numerically using a finite difference-time domain scheme. At first, the pulse appears to leave the domain without reflection. However, as time evolves, the exponential instability emerges. The evolution of the instability in the figure is not primarily governed by numerical factors, such as rounding errors or phase errors. The problem is numerically resolved, and the unstable mode emanates from the initial conditions of the problem, that is, the initial condition has a component of the form $e^{\frac{r}{R_2}}/r$.

3.2. Absorbing right boundary. The next example is similar to the first one, with an absorbing boundary condition also to the right. In the one-dimensional, spherically symmetric case, the right boundary conditions takes the form

$$-\frac{\partial p}{\partial t} = \frac{\partial p}{\partial r} + \frac{p}{R_2}, \quad r = R_2, \tag{13}$$

which is equivalent to the first order spherical ABC used in[2]. With the same ansatz as before, we get the relations

$$s\left(A\frac{e^{-sR_1}}{R_1} + B\frac{e^{sR_1}}{R_1}\right) = -A\frac{se^{-sR_1}}{R_1} + B\frac{se^{sR_1}}{R_1}, \tag{14a}$$

$$s\left(A\frac{e^{-sR_2}}{R_2} + B\frac{e^{sR_2}}{R_2}\right) = A\frac{se^{-sR_2}}{R_2} - B\frac{se^{sR_2}}{R_2}, \tag{14b}$$

between A, B and s. From (14a) we have $s = 0$ or $A = 0$. Similarly, (14b) gives $s = 0$ or $B = 0$. Obviously, for $s \neq 0$ the equation only has the trivial solution $A = B = 0$.

For $s = 0$, however, Eqn. (12) satisfies Eqn. (7) and (13) for $C = 0$ and any D. We thus have

$$R(r) = \frac{D}{r},$$

and hence

$$p(r,t) = \frac{D}{r}. \tag{15}$$

We have found a nonzero eigensolution to the problem, with a corresponding zero eigenvalue. This means that in a time domain simulation, there may, depending on the initial conditions, be a disturbance constant in time left when the transient part of the wave has decayed.

3.3. Open right boundary. In the last example, the right boundary condition is changed to $p(R_2) = 0$, which is an approximation of the boundary condition at the open end of a narrow waveguide. (In reality, the situation is more complicated, since an open-ended waveguide radiates sound to the surrounding medium. An example of a situation where a Dirichlet condition is very accurate is at the interface between water and air.) The same procedure as earlier gives the equation

$$\begin{aligned} s\left(A\frac{e^{-sR_1}}{R_1} + B\frac{e^{sR_1}}{R_1}\right) &= -A\frac{se^{-sR_1}}{R_1} + B\frac{se^{sR_1}}{R_1} \\ A\frac{e^{-sR_2}}{R_2} + B\frac{e^{sR_2}}{R_2} &= 0 \end{aligned}$$

This equation only has only the trivial solution, for all values of s, which is exactly what one would like for a system like this; There are neither growing nor remaining modes in the domain.

From a physical point of view, it may at first glance seem curious that the examples of sections 3.1 and 3.3 behave so differently. In both cases, the power reflection coefficient, defined as the ratio between reflected and incident power, of the right boundary is one. Yet the first example is unstable, whereas the second example is not.

4. A two-dimensional model example. This section presents a two-dimensional example where an ABC is imposed on a convex surface. A simulation of this kind was presented in [4], where time-domain data was used to compute high resolution input impedance spectra of acoustical horns. The simulation involved a broad band acoustic pulse that was fed into the horn to be investigated. By recording the acoustic pressure ($p_{in}(t)$) and normal component ($v_{in}(t)$) of the particle velocity at the input end of the horn during the simulation, the input impedance $Z_{in}(\omega) = S^{-1}p_{in}(\omega)/v_{in}(\omega)$ was calculated after Fourier transforming $p_{in}(t)$ and $v_{in}(t)$. The aim of imposing a non-reflecting boundary condition on part of the domain was to minimise the reverberation time of the system, thus decreasing the computational work of the simulation. The method of carrying out a time-domain simulation of a quickly transient process in order to obtain frequency domain data is also sometimes used by the electro-magnetic community.

Figure 2 shows a flaring waveguide with both ends terminated by spherical caps. The waveguide is axi-symmetric, and made of a sound-hard material modelled by the Neumann condition $\partial p/\partial n = 0$ at the upper and lower boundaries. The interior of the

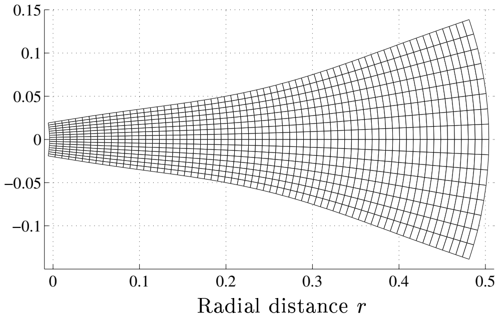

FIG. 2. *A two dimensional waveguide with convex terminations.*

waveguide has been discretised using a curvilinear, orthogonal mesh on which wave propagation can be simulated employing a finite difference–time domain method. In the experiments, an acoustic pulse

$$p_0(t) = -(1+\cos(t-R_1))\sin(t-R_1), \quad 0 \le t \le 2\pi,$$
$$p_0(t) = 0, \quad t > 2\pi$$

was fed in through the left boundary. $p_0(t)$ is the part of the acoustic pressure at the centre of the left boundary emanating from the input pulse. The pulse has compact support in time, and is two times differentiable. The left boundary condition was given by

$$\frac{\partial p}{\partial t} - 2\frac{dp_0}{dt} = \frac{\partial p}{\partial r} + \frac{p}{R_1}, \tag{16}$$

where R_1 is the radius of the spherical cap at the left boundary surface. This boundary condition is equivalent to (7b), with the addition of the forcing term generating the pulse. (Note that $p_0(t)$ is the *right-travelling* part of the pulse, not necessarily equal to the acoustic pressure at R_1, which is the sum of the left- and the right-travelling components.)

The right boundary condition was chosen to be respectively sound-hard, absorbing, and finally pressure release (Dirichlet condition). Figure 3–5 shows the acoustic pressure at the centre of the left boundary surface as a function of time. The physical constants in the simulation have been normalised, and the time step is dictated by the CFL-condition on the smallest grid cells of the domain. To get an idea about the time scale, the number of time steps required for a wave to travel from the left to the right boundary is around 800. Regardless of what boundary condition is imposed at the right boundary, the acoustic pressure at the left boundary will be the same before the arrival of the pulse reflected at the other end of the waveguide.

In the case with an absorbing right boundary, the acoustic field can be expected to decay quickly in the waveguide. As Fig. 4 shows, this is also what happens in the simulation. Shortly after the input pulse has left the left boundary, a weak reflection can be observed. This reflection can be attributed to acoustic energy trapped in the flaring waveguide. The remaining stationary mode corresponding to Eqn (15) is zero due to the choice of a zero-mean test pulse that is symmetric around $t = \pi$.

If a pressure release condition is imposed at the right boundary, all the energy that reaches the boundary is reflected back into the domain. As Fig. 5 shows, the reflected pulse has been phase shifted $-\pi$ radians. The rapid but quickly transient oscillations, visible after the return of the main pulse, are due to multiple reflections between the right boundary and the sudden flare of the waveguide approximately around $r = 0.25$.

Of the three examples, the case with a sound-hard right boundary is physically actually the most easily realisable situation. A first order ABC of Engquist-Majda type is exact only for waves of perpendicular incidence, and the physical difficulties in imposing a pressure release boundary conditions have already been discussed. A sound-hard boundary is, on the other hand, very easily constructed by merely constructing the waveguide walls of a reasonably dense material. Nevertheless, as Fig. 3 shows, the simulation is unstable. The input wave, the trapped waves and the wave reflected at the right boundary without phase shift can be observed as expected also in this case.

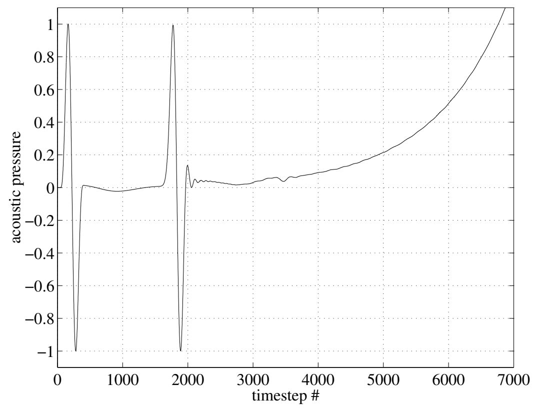

FIG. 3. *Pressure at centre of the left boundary with $p_n = 0$ at the right boundary.*

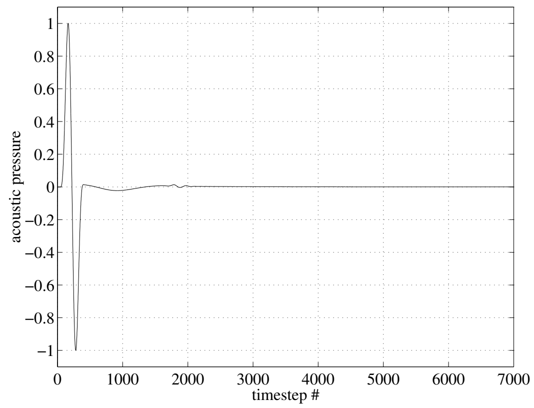

FIG. 4. *Pressure at centre of the left boundary with right boundary absorbing.*

5. Admissible shapes of absorbing boundaries. We have seen that convex absorbing boundary conditions in some cases give rise to instabilities, whereas they

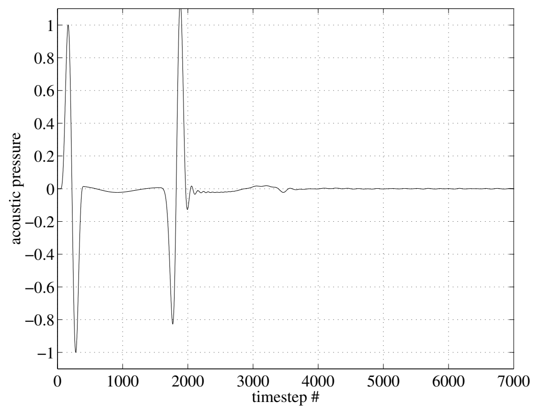

FIG. 5. *Pressure at centre of the left boundary with $p = 0$ at the right boundary.*

may work in other cases. Whether or not they do so depends on other properties of the problem at hand, mainly the other boundary conditions.

From the foregoing discussion, one could easily draw the conclusion that absorbing boundaries of convex shapes cannot be used – at least not guaranteeing stability of a simulation in the general case. Figure 6 shows a case where a convex absorbing boundary could be preferential. The object at hand is embedded in a small computational domain Ω. In order to keep this domain small, part of the boundary is spherical.

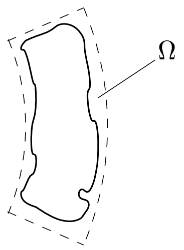

FIG. 6. *An embedded object.*

In reality, the shape of the boundary alone is not the crucial point. We have seen that a boundary condition capable of absorbing converging conical waves is generally not admissible. However, if one would construct a boundary condition on a convex surface, that is capable of absorbing planar wavefronts, the situation would be completely different. The somewhat hypothetical geometry of Fig. 7 illustrates the argument. On Γ_1, a boundary condition with the above mentioned properties is imposed. The left-travelling wavefronts indicated at x_ℓ will, by construction of the boundary condition, leave the domain Ω without reflection. Constructing and implementing such a boundary condition is technically somewhat problematic, especially at the corners between Γ_1 and Γ_2, but nonetheless possible. For the actual solution of the Helmholtz equation on Ω, one can imagine a finite element method to be used, for instance. With this arrangement, left travelling waves will pass the imagined surface S_1 without reflection. The part of Ω to the left of S_1 might thus be represented by a flat Cartesian absorbing boundary condition, which is known to give a well posed

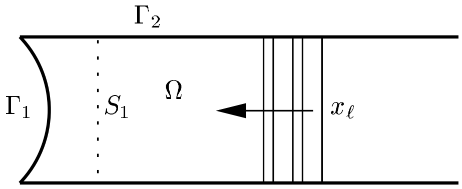

FIG. 7. *Channel with convex ABC.*

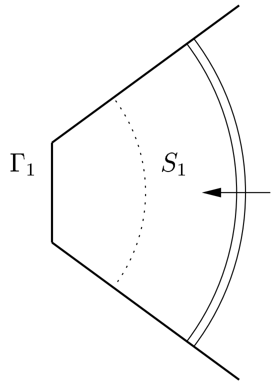

FIG. 8. *Conical waveguide with planar ABC.*

mathematical problem, and also a physically stable system, according to the definition used here.

The inversion of the previous argument is that also an ABC applied on a flat boundary may invoke instabilities in certain cases. Consider the geometry in Fig. 8. It consists of a frustum, on which an ABC is imposed on Γ_1. The ABC is perfect in the sense that the reflection coefficient is zero for all angles if incidence. On the lateral surface of the frustum, again the Neumann condition $\partial p/\partial n = 0$ is imposed. This time, the region between Γ_1 and the spherical cap S_1 can be replaced by an absorbing boundary condition that we know may lead to dynamic instabilities.

6. Conclusions. It has been shown that a careless choice of the shape of an absorbing boundary may lead to dynamic instabilities. These instabilities are the result of non-physical assumptions about the acoustical situation at hand. The unphysical assumption here is that spherical waves can somehow enter a converging cone, and be absorbed completely without reflection. The tip of a cone can be filled with an absorbing tissue or some other damping material, but in reality some reflection will take place at the interface between the air in the cone and the damping material.

If the unphysical boundary condition investigated here leads to an exponential growth of the solution or not depends on the other boundary conditions of the problem.

An important conclusion is that it is not meaningful to look for alternative formulations of absorbing boundary conditions on convex surfaces, with the property that converging spherical waves are absorbed in the classical sense. By this is meant that the symbol of the boundary operator is analytic. For propagating waves, that is for real ω (corresponding to purely imaginary values of s), the absorbing boundary condition must have the form $i\omega p = \partial p/\partial r + p/R_1$ in order for propagating waves to be transported out of the domain.

Instead, the physical situation has to be re-modelled. In certain cases, such as in [4], the violation of the passivity constraint is not detrimental for the computation of the interesting property (in this case the input impedance), as long as the acoustic pressure in the investigated object does not grow exponentially. If this is the case or not is, however, a matter that depends on the acoustical damping in the rest of the domain.

REFERENCES

[1] D. P. Berners. *Acoustics and signal processing techniques for physical modeling of brass instruments.* PhD thesis, Stanford University, 1999.

[2] B. Engquist and A. Majda. Absorbing Boundary Conditions for the Numerical Simulation of Waves. *Mathematics of Computation*, 31:629–651, 1977.

[3] B. Gustafsson, H. O. Kreiss, and J. Oliger. *Time dependent problems and difference methods.* John Wiley & Sons, New York, 1995.

[4] D. Noreland. A Numerical Method for Acoustic Waves in Horns. *Acta Acustica united with Acustica*, 88:576–586, 2002.

[5] F. L. Teixeira. Sytematic derivation of anisotropic PML absorbing media in cylindrical and spherical coordinates. *IEEE Microwave and guided wave letters*, 7(6):371–373, 1997.

[6] F. L. Teixeira. On causality and dynamic stability of perfectly matched layers for FDTD simulations. *IEEE Transactions on microwave theory and techniques*, 47(11):775–785, 1999.

[7] F. L. Teixeira. Conformal PML-FDTD schemes for electromagnetic field simulations: A dynamic stability study. *IEEE Transactions on antennas and propagation*, 49(6):902–907, 2001.

[8] S. V. Tsynkov. Numerical solution of problems on unbounded domains: A review. *Appl. Numer. Math.*, 27:465–532, 1998.

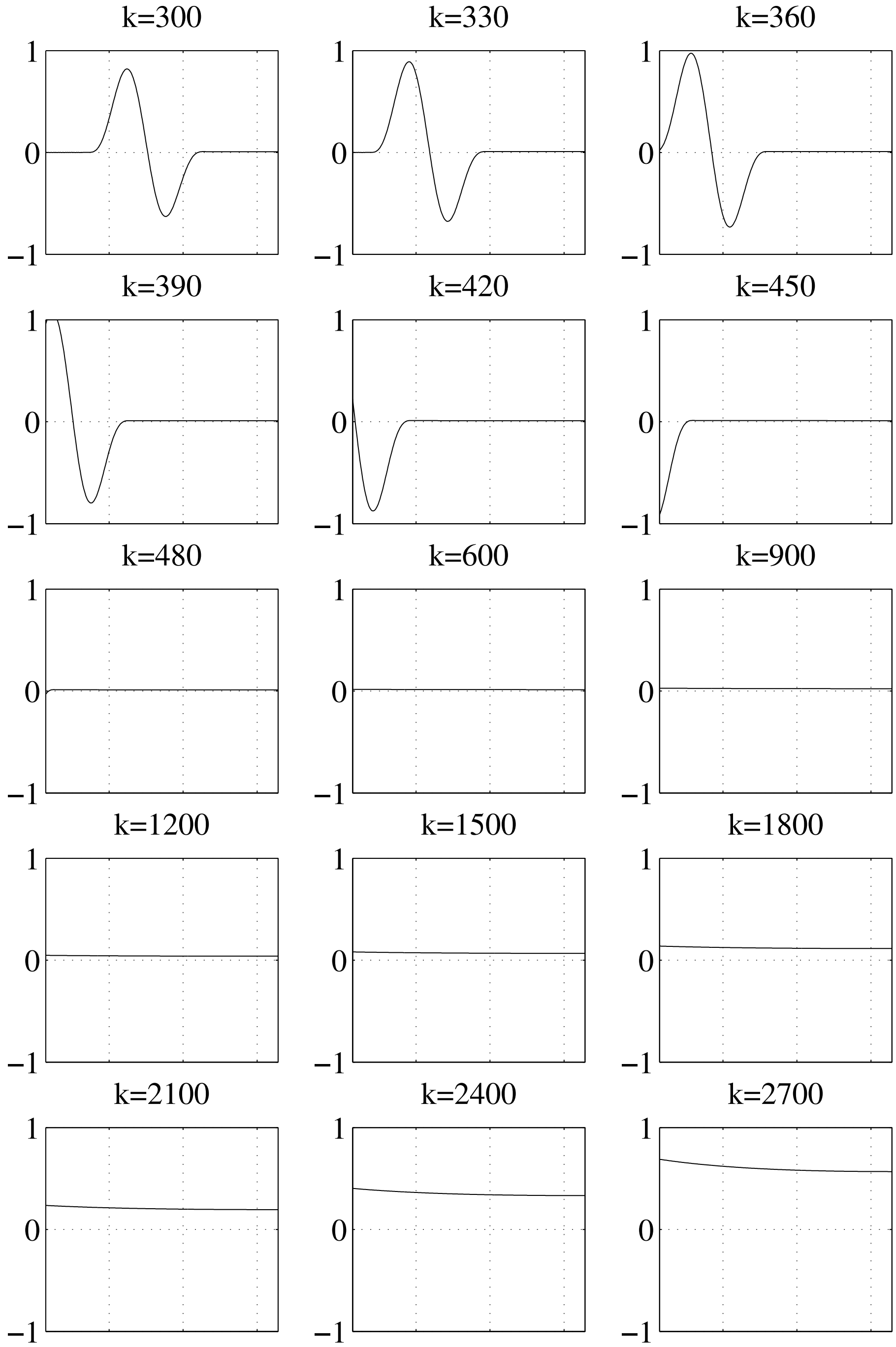

Fig. 9. *Time evolution of a converging wave. The frames show the acoustic pressure as a function of radial distance for different time steps during the simulation (note that the time between frames varies). The number of time steps required for the pulse to travel from one end of the domain to the other is 280.*